

# Development of a Low Speed Linear Generator for use in a Wave Energy Converter

J. Ribeiro<sup>1</sup> and I. Martins<sup>1</sup>

<sup>1</sup> Department of Electrical and Electronics Engineering  
I.S.E., University of Algarve  
Campus of Penha – Faro, 8000 Faro (Portugal)

Phone/Fax number: +351 289 800165, e-mail: [joseribeiro.eee@gmail.com](mailto:joseribeiro.eee@gmail.com), [imartins@ualg.pt](mailto:imartins@ualg.pt)

**Abstract.** One of the main advantages of ocean waves as resource for electrical energy production is its high energy density. Several methods have been proposed for the conversion of ocean wave mechanical energy into electrical energy. One such method consists in the use of a direct drive linear generator enclosed inside a floating element. The generator is driven by a mass-spring system, which oscillates due to the ocean wave's movement. In this paper are presented the study, development, and dynamic simulation of a linear tubular synchronous low speed permanent magnet generator, for use in a wave energy conversion system. The generator was dimensioned using a finite element analysis tool. The wave energy converter dynamic model, mechanical and electrical, was developed to evaluate its response. To validate the generator's dimensioning and dynamic model, its prototype was built. The dynamic model simulation results and the prototype's experimental results are presented.

## Key words

Dynamic Model, Finite Element Analysis, Linear Tubular Synchronous Permanent Magnet Generator, Wave Energy, Wave Energy Conversion System

## 1. Introduction

The countries whose energy markets are highly dependent on hydrocarbons are subjected to the price variations (of the hydrocarbon fuels) that have occurred in the last years, as well to possible political and military conflicts in the producing countries that may cause supply disruption. One way to immunize a country's energy market from instability consists on the energy sources diversification. If the energy sources are renewable it's also possible to reduce green house gases emissions, increasing the energetic independence at the same time.

Energy extraction and conversion from the ocean waves may come to contribute to the objectives mentioned above. That's due to the wind generated waves high energy density, the highest of the available renewable energy sources [1]. Nevertheless, the exploration of this

form of energy still faces several technological challenges, which may be surpassed through research and development.

Although it isn't considered yet a mature technology, several years of research and development have resulted in a myriad of wave energy devices. These devices can be classified according to their location or operating principle. Depending on the location of the installation, wave energy devices can be divided into three categories [2]: shoreline, nearshore, or offshore. According to their operating principle, wave energy devices can also be divided into three categories [3]: oscillating water columns, overtopping devices, or wave activated bodies.

The wave energy device, whose study and development is presented in this paper, is a wave activated body, meant to be installed near the shore or offshore. This device consists, essentially, in a floating element (buoy) that contains in its interior all the necessary elements to convert the wave's mechanical energy into electrical energy [4], as schematized in Figure 1. This system is meant to be anchored to the sea bed through a single mooring, which may also serve as a guide to the underwater electrical cable. The monitoring of this kind of system could be accomplished through wireless communications or fiber optics.

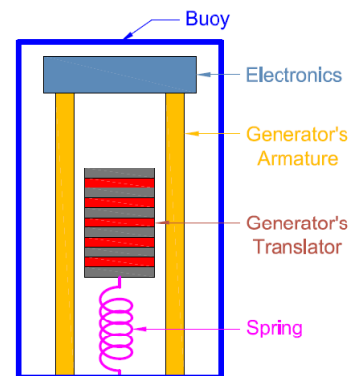


Fig. 1. Longitudinal cut of the proposed wave energy converter.

For the electrical energy generating element, a linear tubular permanent magnet synchronous generator is proposed. This electrical machine is also slotless and its permanent magnets are axially magnetized. This topology presents several advantages and some disadvantages as well.

One of the advantages of a slotless machine is the possibility to increase the outer diameter of the permanent magnet field system, as the available space for copper increases, due to the elimination of the stator's teeth [5]. Alternatively, the copper area can be increased, thus increasing the total current in the machine's coils, for the same current density. However, this total current increase shouldn't be exaggerated, as the removal of the armature's teeth also means the loss of a cooling vehicle [5]. The electromotive force harmonic's content is also inferior in a slotless machine. In an electrical machine of this kind is also possible to use laminated steel of inferior quality, due to the low density of magnetic flux in the armature's core. For low speed machines the armature's core doesn't even need to be laminated, as the losses due to eddy currents are very small. Nevertheless, the suppression of the armature's teeth is only possible due to the use of high magnetic energy permanent magnets [5], usually neodymium.

The linear tubular topology also presents some advantages, mainly its easy construction and the elimination of the need to use motion conversion mechanisms, as would be required if the employed generator were to be a rotating machine, diminishing the mechanical losses and increasing reliability.

This paper deals with the dimensioning and dynamic modeling of an ocean wave energy system. The buoy is crudely sized, as is only intended to allow the dynamic simulation of the generator integrated in a floating element. The generator is dimensioned using analytical equations, and finite element analysis with a third party software package (FEMM). The system's response to a sinusoidal ocean wave is also analyzed, for several load values. The prototype's test results are compared with the generator model results, in order to validate the mathematical model.

## 2. Generator's Dimensioning

The proposed generator's topology is, as referred, a linear tubular permanent magnet synchronous electrical machine, where the armature's length is greater than the translator's length in a proportion of 18 to 5. The generator is designed as a 3Phase machine, but all of its coils form independent phases connected to an uncontrolled rectifier, in a total of 54 phases. The electrical machine's longitudinal cut is represented in Fig. 2, where the drawing shows a machine with equal lengths of the armature and translator due to page space issues only. The ABC letters on the armature's coils represent the electrical phase according to its angle ( $0^\circ$ ,  $120^\circ$  and  $-120^\circ$ ), and the + and - signs represent the coil's winding direction. The translator's magnets are axially

magnetized, integrating a magnetic field system that is glued together with epoxy, and slides along a central shaft, made of non-magnetic metal.

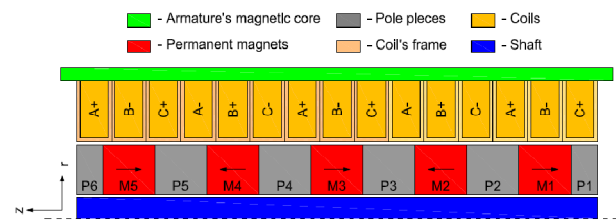


Fig. 2. Generator's longitudinal cut.

The choice to use every coil as an independent phase has an advantage over the alternative: connect in series all the coils with the same electrical angular displacement. That's due to the fact that, since the armature's length is greater than the translator's length, there are coils that won't be magnetically excited while others are. If coils with the same angular displacement were to be connected in series, this would create a problem from the ohmic losses point of view.

The generator is sized in 3 steps: armature's magnetic core sizing, magnetic field system sizing, and coil's sizing. To that effect, the generator's magnetic circuit is reduced to an electric equivalent circuit, shown in Fig. 3, where the permanent magnet is modeled through a voltage source in series with its reluctance [6]. Since the generator is symmetrical, only a machine's portion is considered.

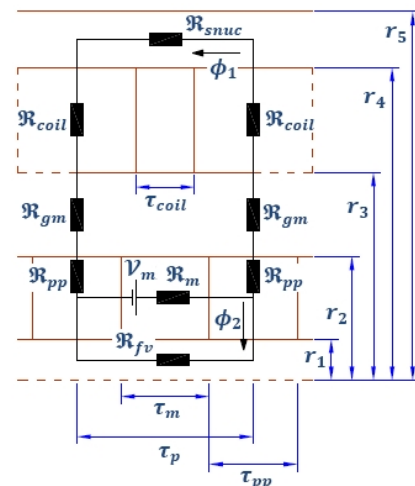


Fig. 3. Generator's magnetic circuit electric equivalent.

As the machine's magnetic circuit components are simple geometric forms, it's very easy to calculate the various magnetic reluctances using expression (1). The magnet's equivalent voltage source is expressed by (2) [6].

$$\mathfrak{R} = \int \frac{l}{\mu A} dA \quad (1)$$

$$\mathcal{V}_m = H_c \tau_m \quad (2)$$

Using the *Kirchhoff Voltage Law*, the equivalent circuit in Fig. 3. can be described through the system of equations (3).

$$\begin{cases} -\mathcal{V}_m + \mathfrak{R}_m(\phi_1 + \phi_2) + 2\mathfrak{R}_{pp}\phi_1 + \\ 2\mathfrak{R}_{gm}\phi_1 + 2\mathfrak{R}_{bob}\phi_1 + \mathfrak{R}_{snuc}\phi_1 = 0 \\ -\mathcal{V}_m + \mathfrak{R}_m(\phi_1 + \phi_2) + \mathfrak{R}_{fv}\phi_2 = 0 \end{cases} \quad (3)$$

$$\phi_m = \phi_1 + \phi_2$$

The generator's magnets are formed by several magnets stacked together. Since they were pre-acquired, it's only possible to calculate the magnet's length  $\tau_m$ , as its internal  $r_1$  and external  $r_2$  radius are fixed. As the magnet's material is known (NdFeB N42), it's possible to find its best operating point: operation at maximum magnetic energy. Imposing the coil's height ( $r_3$  and  $r_4$ ) and the maximum intended magnetic flux density in the armature's magnetic core  $B_{snuc}$ , it's possible to determine the core's outer radius  $r_5$  using expression (4), where  $B_m$  represents the magnet's flux density at the intended operating point.

$$r_5 = \sqrt{\frac{B_m(r_2^2 - r_1^2)}{B_{snuc}} + r_4^2} \quad (4)$$

Knowing all the machine's radiuses, and assuming that the magnet's length is equal to the pole piece length ( $\tau_m = \tau_{pp}$ ), the polar length  $\tau_p$  can be determined using the system of equations (3).

Having determined the magnetic circuit dimensions, the final step is to calculate the coil's number of turns and wire diameter. To that effect, finite element analysis was used to precisely determine the magnetic flux embracing each coil. This measure was taken because, although the equivalent circuit in Fig. 3 is very good for sizing the magnetic circuit, as proved later by FEA, it offers a very poor approximation for a coil's linkage flux. That poor approximation is due to the absence of teeth in the armature, which means that a good portion of the pole's magnetic flux constitutes leakage flux.

Knowing a coil's magnetic flux, admitting a nominal speed of  $0.5 \text{ m/s}$ , and a peak voltage drop of  $20 V_{pp}$  per phase, the coil's number of turns and wire diameter can be determined using the Faraday Law, in the form of (5), where  $\hat{\phi}$  represents the maximum flux per coil.

$$\hat{E}_{emfcoil} = \hat{\phi} N \frac{\pi}{\tau_p} v_{gen} \quad (5)$$

After the generator's dimensioning (main properties abridged in Table 1), FEA was used to verify the said dimensioning, with two main objectives in mind: identify possible areas of the permanent magnets in risk of demagnetization, and the assessment of the longitudinal

end effects influence in the machine's electromotive force (emf).

Table 1. Generator's main properties.

Symbol	Description	Value
$r_1$	magnet internal radius	7.5 mm
$r_2$	magnet external radius	22.5 mm
$r_3$	coil internal radius	24.5 mm
$r_4$	coil external radius	36 mm
$r_5$	generator external radius	40 mm
$N$	coil turns	478
$d_{wire}$	wire diameter	0.40 mm
$\tau_m$	magnet length	16 mm
$\tau_p$	polar length	32 mm
$N_{permMag}$	number of magnets	5
$N_{conTrif}$	number of 3Phase sets	18
$R_{phase}$	phase resistance	11.85 $\Omega$
$L_{aa}$	phase self inductance	0.03 H
$I_f$	phase nominal RMS current	0.3863 A
$P_{emf}$	total nominal RMS power	81.95 W
$F_{em}$	nominal maximum force	116.32 N

To meet the first objective, the magnetic field system's flux density graphic was plotted, shown in Fig. 4. In the Fig. 4 graphic, delimited by black rectangles, it's possible to observe that only 2 extremely small portions of the PM present a low magnetic flux density, around 0.2 T. Since the armature's magnetic field has very low amplitude compared to the magnet's field, there's no risk of demagnetization of the PMs.

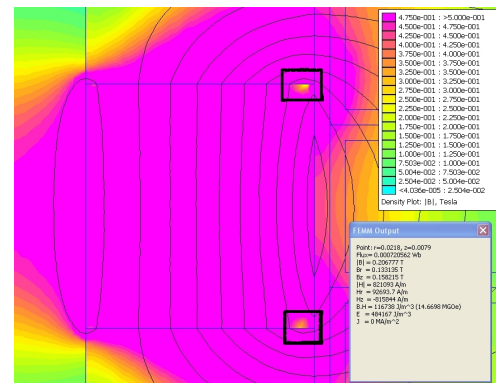


Fig. 4. PM's magnetic flux density plot.

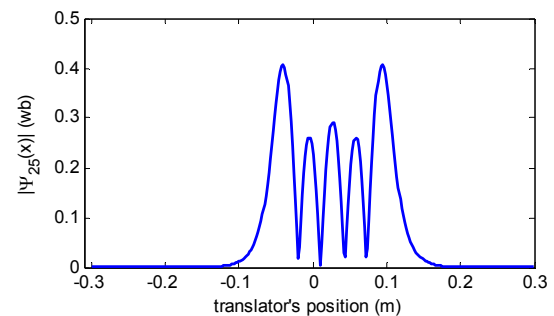


Fig. 5. Phase 25 linkage flux absolute value vs. translator's position.

The second objective, the analysis of the end effects impact in the electromotive force, was met through the calculation, by FEA, of the linkage flux in all of the generator's phases. As can be seen in phase's 25 linkage flux absolute value vs. translator position plot, depicted in Fig. 5, the magnetic flux distribution in the armature is not constant, presenting with different amplitudes that can have a difference of more than 25%. This uneven magnetic flux distribution should've been accounted for in the generator's design, and could be lessened with an even PM number [1].

The generator's dimensioning was achieved with the implementation of all of the necessary calculations in a Matlab script, completely automating the process. All finite element analyses required for this task were performed by FEMM, integrated with the developed script.

### 3. Dynamic Model

The wave energy system's dynamic model is composed by two independent, but interconnected, models: the buoy and generator's mechanical model, and the generator's electric model.

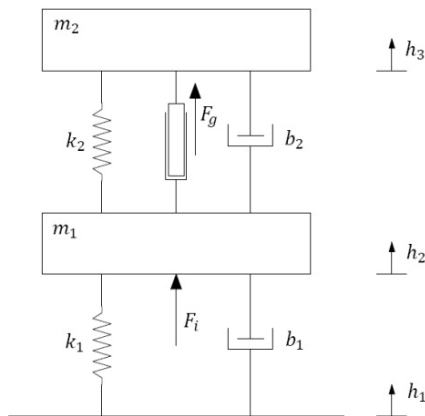


Fig. 6. System's 2 degree of freedom equivalent mechanical model.

The system's mechanical model is obtained through its representation in the equivalent 2DOF model in Fig. 6, where  $m_1$  represents the entire buoy's still masses and  $m_2$  represents the buoy's mobile masses. The  $b_1$  parameter represents the hydrodynamic friction coefficient,  $k_1$  represents the Archimedes force coefficient, and  $k_2$  represents the generator's spring stiffness coefficient.  $F_g$  represents the generator's electromagnetic force and  $h_1$  is the wave's surface displacement. The  $F_i$  e  $b_2$  parameters aren't used, as they were only included to make the system more comprising.

The 2DOF system in Fig. 6 can be governed by the equations in (6). This system of equations led to the mechanical model state space matrix equations

development. The state space equations were in turn implemented in Simulink.

$$\begin{cases} m_1 \ddot{h}_2 + k_1(h_2 - h_1) + b_1(\dot{h}_2 - \dot{h}_1) + \\ k_2(h_2 - h_3) + b_2(\dot{h}_2 - \dot{h}_3) + F_g - F_i = 0 \\ m_2 \ddot{h}_3 + k_2(h_3 - h_2) + b_2(\dot{h}_3 - \dot{h}_2) - F_g = 0 \end{cases} \quad (6)$$

For the generator's electric model two distinct approaches were taken. The first models the machine as a permanent magnet DC generator, as the sized generator supplying a load through a rectifier can be seen that way. The second approach models the generator as a permanent magnet 54Phase synchronous generator. Both models present advantages and disadvantages.

The generator's DC model can be represented by the equivalent circuit in Fig. 7, whose inductance and resistances are reflected to the rectifier's output.

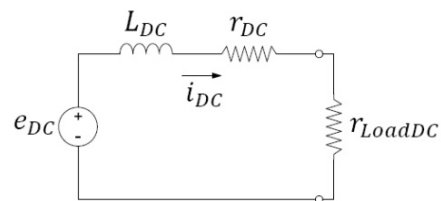


Fig. 7. Generator's DC model equivalent circuit.

The equivalent circuit shown in Fig. 7 can be described by equations (7) and (8), where  $k\phi_{DC}$  represents the machine's force coefficient. This parameter was determined through FEA, and its plot is shown in Fig. 8. The DC model's equations were implemented in Simulink, where  $k\phi_{DC}$  was implemented by a look-up table.

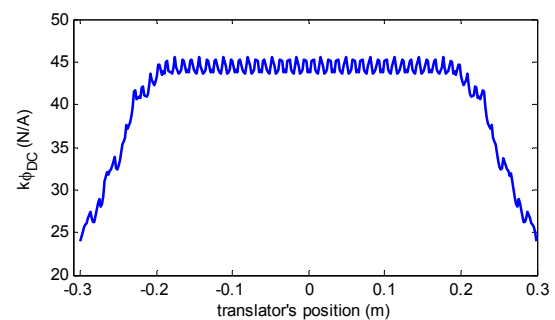


Fig. 8.  $k\phi_{DC}$  vs. translator's position.

$$\frac{di_{DC}}{dt} = -\frac{r_{DC}}{L_{DC}} i_{DC} + \frac{k\phi_{DC}}{L_{DC}} v_{gen} - \frac{r_{LoadDC}}{L_{DC}} i_{DC} \quad (7)$$

$$F_{eDC} = k\phi_{DC} \times i_{DC} \quad (8)$$

The DC machine model presented for the generator has the advantage to be very fast to calculate and requires low computing resources for execution. Whoever, the quantity of information available to the user is very limited; as it only can be obtained data from the



rectifier's output. The second proposed model has as advantage the large quantity of information available to the user, per phase, and the disadvantage to require a large quantity of computing resources to calculate all of the model's parameters:  $3 \times 54$  look-up tables, calculated through FEA.

The second proposed model, generator as a synchronous machine, uses the equivalent circuit per phase in Fig. 9, and can be described by expression (9), where  $r_{La}$  represents the load per phase. The  $e_{a lump}$  source concentrates the phase's emf and the phase's inductive voltage drop.

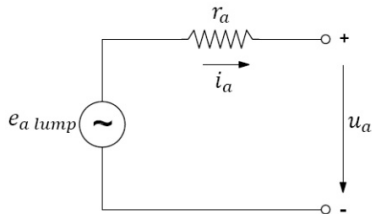


Fig. 9. Generator's synchronous machine model equivalent circuit.

$$i_a(t) = \frac{\frac{d}{dx}\psi_a(x, i_a)}{r_a + r_{La}} v_{gen} \quad (9)$$

Along with other equations, equation (9) was implemented in Simulink, and its block diagram per phase is shown in Fig. 10. This model per phase calculates several parameters, like the current, instant power on the load and phase resistance, phase's voltage drop, phase's emf, and  $e_{a lump}$ . The  $\frac{d}{dx}\psi_a(x, i_a)$  and  $\frac{d}{dx}\psi_{a mag}(x)$  parameters are implemented in the form of look-up tables.

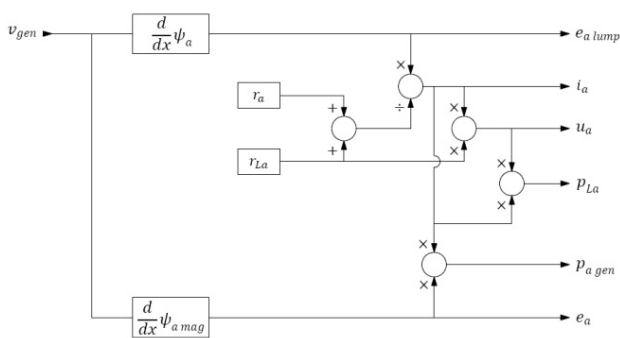


Fig. 10. Generator's synchronous machine block diagram.

The synchronous generator force model is the direct implementation in Simulink of look-up tables, one per phase  $F_{e a}(x, i_a)$ , whose data was obtained through FEA. Figure 11 shows phase 27 force 'map'  $F_{e 27}(x, i_{27})$ .

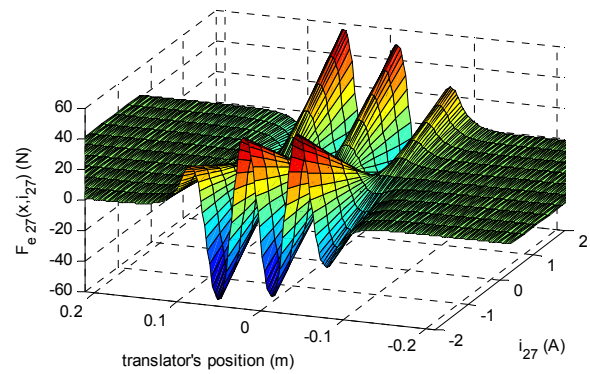


Fig. 11. Generator's phase 27 force 'map'  $F_{e 27}(x, i_{27})$ .

#### 4. Dynamic Response

Having completed the system's model development and implementation, its response to a pure sinusoidal wave was analyzed. This had the main objectives of determining the designed buoy's efficiency, and comparing the data provided by the models against the project data and the built generator. In a first instance the system was simulated for 3 different operating frequencies: system's natural frequency, a frequency below the natural frequency, and a frequency above the natural frequency. In a second instance the system's response was analyzed for several different electric load values.

The buoy's efficiency, that is, the ratio between the captured energy and the energy supplied to the generator, was found to be around 1.3%, for the system's resonance frequency. This low value of efficiency is explained by the generator's mobile mass  $m_2$  low value. A five times increase in  $m_2$  led to an almost five times increase in the buoy's efficiency. Also, the buoy's diameter is several times larger than the generator's diameter, and the energy captured by the buoy depends on its diameter.

Comparing the data provided by the generator's models against the project initial parameters, a maximum difference of 11% was determined. This somewhat large difference is due to the electrical machine's longitudinal end effects that have a considerable impact in the generator's performance, and weren't compensated for in the project phase.

Simulating the system for several different electric load values, the generator's efficiency plot is obtained, and shown in Fig. 12. This plot shows that higher the load resistance, higher the machine's efficiency. This is due to the brake effect that the generator exerts on its own translator. A higher resistance means a lower current, and a lower reaction force; therefore the translator's mass has a movement with higher amplitude for the same power input. A higher performance is obtained with low currents (low ohmic losses in the armature) and high voltage drops at the machine's terminals. However, there is a limit to the load's value, as marked in Fig. 12, since

the translator's amplitude of movement cannot exceed its physical limitations.

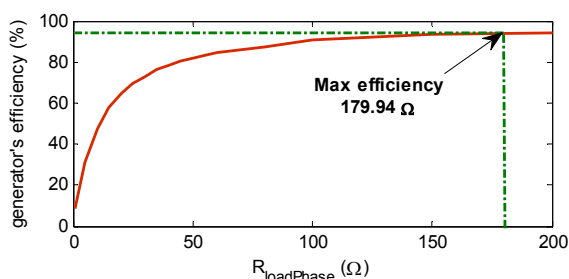


Fig. 12. Generator's efficiency vs. phase load resistance.

## 5. Experimental Results

To validate the generator's developed mathematical model its prototype was built, and some parameters were measured. The machine's response to its translator movement was also analyzed.

The measured physical parameters are the coils resistance and self inductance (without translator). The minimum measured resistance value is  $12.6\Omega$ , and the maximum measured resistance value is  $13.4\Omega$ . This represents a maximum difference of 19% relatively to the calculated value. The minimum measured self inductance value is  $19.57mH$ , and the maximum measured self inductance value is  $21.9mH$ . This represents a maximum difference of 7.3% relatively to the calculated value ( $21.0mH$ ).

These differences between the measured and calculated values can be attributed to the fact that the built machine didn't follow the project specifications to the detail, as the prototype was built in an artisanal way, due to budget limitations. As such, the prototype's magnetic circuit is somewhat different from the project's magnetic circuit, which means different values of inductances. However, since the generator was designed to operate at very low speeds, hence low current frequencies, the inductance value has little impact on the machine's performance.

Moving the translator along its shaft, the generator's phase 27 no load voltage drop was measured. The measured wave form is depicted in Fig. 13. For the same operating conditions, the same waveform was also obtained from the generator's model. The difference between the measured peak voltage and the calculated peak voltage was found to be around 2.2%.

Although the built prototype presents large differences between its measured parameters and its project parameters, several comparisons between the generator's model and its prototype test data showed a difference no greater than 5.3%. As such, the generator can be accurately modeled by the developed tool.

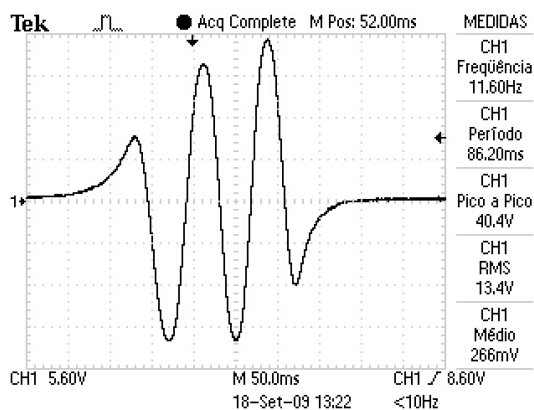


Fig. 13. Generator's phase 27 emf.

## 6. Conclusion

This paper deals with the dimensioning and modeling of a wave energy extraction and conversion system, more particularly of its electrical generator. It was showed that the generator can be accurately modeled by the developed dynamic model. The buoy's efficiency can be increased through the increase of the translator's mass. The electric machine efficiency can be optimized through the use of current control, i.e. load control. This control allows the produced energy maximization, and also ensures that the generator's operating characteristics aren't surpassed during operation.

In future work the buoy's design and respective dynamic model should be improved, to maximize its accuracy. It also should be developed the electronic load control to maximize the power output.

## Acknowledgements

Acknowledgment is due to the author of the utilized finite elements analysis program Finite Element Method Magnetic (FEMM).

## References

- [1] Danielsson, O., Wave Energy Conversion – Linear Synchronous Permanent Magnet Generator, Ph.D. Thesis, Uppsala University, Uppsala (2006), pp. 13-80.
- [2] Wave Energy Center, Potencial e Estratégia de desenvolvimento da energia das ondas em Portugal, WEC, Portugal (2004), pp. 9-10.
- [3] Harris, R.E., Johanning, L. and Wolfram, J., Mooring systems for wave energy converters: A review of design issues and choices, Edinburgh (200?), pp. 1-10.
- [4] Luan, H., Onar, O.C. and Khaligh, A., Dynamic Modeling and Optimum Load Control of a PM Linear Generator for Ocean Wave Energy Harvesting Application, IEEE Applied Power Electronics Conference and Exposition, APEC 2009, pp. 739-743.
- [5] Miller, T.J.E., Brushless Permanent-Magnet and Reluctance Motor Drives. Oxford University Press, Glasgow (1993), pp. 115-117.
- [6] Furlani, E.P., Permanent Magnet and Electromechanical Devices, Academic Press, New York, (2001), pp. 153-161.